Soft Matter

Cite this: *Soft Matter*, 2011, **7**, 7386

www.rsc.org/softmatter

PAPER

Fabrication and evaluation of reduction-sensitive supramolecular hydrogel based on cyclodextrin/polymer inclusion for injectable drug-carrier application

Jiahui Yu,[a] Honglei Fan,[b] Jin Huang*[ab] and Jinghua Chen[bc]

Received 11th March 2011, Accepted 22nd May 2011
DOI: 10.1039/c1sm05426k

Supramolecular hydrogels based on cyclodextrin/polymer inclusion are an emerging injectable biomaterial for drug controlled-release and cell capsulation. Although the pH- and temperature-sensitivity has been focused on contributing to intelligence, the system sensitive to physiological reduction condition caused by glutathione tripepetide (GSH) has not been reported so far. In this work, novel reduction-sensitive supramolecular hydrogels were, for the first time, fabricated by the inclusion of [poly(ethylene glycol) monomethyl ether]-*graft*-[disulfide-linked poly(amido amine)] (mPEG-*g*-SS–PAA) with α-cyclodextrin (α-CD) in aqueous solution. The reduction-sensitivity was ascribed to the disulfide linker in the SS–PAA main chain while various physical conjugations contributed to a reversible gel–sol transition under shearing as a key of injectable function. The drug release from such a supramolecular hydrogel showed a prominent sustained release profile, and the release rate could further be regulated depending upon the reduction condition. It is worth noting that incorporating a low loading-level of reducing agent did not inhibit the formation of hydrogel. As a result, it became possible to use the reduction-sensitivity to regulate the drug release profile in extracellular milieus and normal tissue. Combined with acceptable cytotoxicity, this kind of reduction-sensitive supramolecular hydrogel based on cyclodextrin/polymer inclusion showed a great potential as an injectable smart biomaterial for the application of drug controlled-release.

1 Introduction

Supramolecular hydrogels based on polymer/cyclodextrin inclusion have attracted great interest as promising injectable biomaterials,[1–3] for applications as drug carriers with a sustained release function,[4–13] or as a cell-encapsulation vehicle with a good biocompatibility.[10,14] In such supramolecular hydrogels, drug loading can simultaneously occur during the gelation process. This not only enhances drug loading-levels, but also avoids structural changes of the drug. In particular, physical encapsulation shows prominent advantages for macromolecular drugs, such as nucleic acids, peptides, proteins and so on. Furthermore, a reversible sol–gel transition functioned as shearing force mainly contributes to an injectable function,[5–13,15–17] and breaks through the limits of the conventional implantable strategy for hydrogels. The shearing-response is originated from physical interactions as the driving forces of gelation and the supporting of hydrogel framework. These physical interactions mainly consist of the hydrophobic interaction between the cyclodextrin inner and the polymer, as well as non-covalent aggregation of (pseudo)poly-rotaxanes formed by the threading of cyclodextrin onto the polymer chain. Furthermore, such physical interactions result in the sensitivity functioned as temperature[5,9,18–23] and pH[23] depending upon the structure of the included polymer chains. In addition, the structural character of the polymer guest, such as the cationic or anionic nature of the uncovered polymer segments, also contributes to the additional stimulus-response properties, such as the sensitivity to temperature,[16] pH[5,9,24] and so on. Such stimulus-response properties of supramolecular hydrogels also provide the essential intelligence required by drug delivery and release. However, this kind of supramolecular hydrogel sensitive to physiological reduction conditions caused by glutathione tripepetide (GSH) has not been reported so far.

The reduction-sensitive polymers have emerged as a fascinating class of intelligent biomaterials, and are especially applied to encapsulate drugs in the forms of nano/micro-gel and micelles for their delivery and controlled-release.[25] With respect to the molecular level, the disulfide linkage is a typical character of reduction-sensitive polymers, and usually locates in main chains, side chains or cross-linkers.[25] A notable fact has been found that the cleavage of the disulfide linkage, due to the thiol–disulfide

[a]*Institute of Drug Discovery and Development, Institutes for Advanced Interdisciplinary Research, East China Normal University, Shanghai, 200062, China. E-mail: huangjin@iccas.ac.cn*
[b]*College of Chemical Engineering, Wuhan University of Technology, Wuhan, 430070, China*
[c]*School of Medicine and Pharmaceutics, Jiangnan University, Wuxi, 214122, P. R. China*

exchange reaction, is sensitive to the reduction conditions in the human body, namely the disulfide bonds show enough stability to a low concentration of glutathione tripeptide (GSH), *ca.* 2–20 μM in body circulation and extracellular milieus, while the disulfide linkage quickly cleaves under high GSH concentration, *ca.* 0.5–10 mM of intracellular condition and 4-fold over normal tissue in tumors.

In this study, the disulfide-linked poly(amido amine) (SS–PAA) containing alkyne focal groups as the main chain was designed to become the origin of reduction-sensitivity. Moreover, considering that a branched structure, such as a grafted comb-type,[20–23] a high-densely double-grafted brush[19] and so on, could improve gelation of the polymers containing a low molecular weight of poly(ethylene glycol) (PEG) segments *via* cyclodextrin inclusion, azide-terminated poly(ethylene glycol) monomethyl ether (mPEG–N_3) was grafted onto SS–PAA by "click" chemistry to produce the guest of comb-like polymer (mPEG-*g*-SS–PAA) for the cyclodextrin inclusion. Subsequently, a novel reduction-sensitive supramolecular hydrogel was fabricated by the inclusion of α-cyclodextrin (α-CD) onto mPEG-*g*-SS–PAA, and the elastic modulus and shear-thinning behavior were investigated for verifying the injection function and evaluating mechanical strength. Based on the reduction-degradation behavior of mPEG-*g*-SS–PAA traced by gel permeation chromatography, the drug-release profiles were measured with bovine serum albumin (BSA) as a model protein drug. Hence, the incorporation of dithiothreitol (DTT) as a reducing agent model and a substitute of GSH was expected to regulate the drug release behavior even at a low reduction concentration, such as extracellular milieus in the normal tissue. Finally, the *in vitro* cytotoxicity of such reduction-sensitive supramolecular hydrogels was evaluated by the MTT method in order to explore their possibility as injectable biomaterials.

2 Experimental

2.1 Materials

Cysteamine hydrochloride, propargyl amine, acryloyl chloride and poly(ethylene glycol) monomethyl ether (mPEG) with M_n of 1900 Da were purchased from Alfa Aesar and used as received. Dithiothreitol (DTT), sodium ascorbate and copper (II) sulfate pentahydrate were purchased from Aladdin. Pristine α-cyclodextrin (α-CD), 3-(4,5-dimethylthiazol-2-yl)-2,5-diphenyltetrazolium bromide (MTT) and bovine serum albumin (BSA) were purchased from Aldrich. All other reagents and solvents were obtained commercially and used as received, unless noted otherwise.

2.2 Cell line and culture

Mouse muscular cell line L929 was supplied from Institute of Biochemistry & Cell Biology, Chinese Academy of Sciences. Cells were cultured in RPMI 1640 (Gibco BRL, Paris, France), supplemented with 10% fetal bovine serum (FBS, HyClone, Logan, Utah), streptomycin at 100 μg mL^{-1}, and penicillin at 100 U mL^{-1}. All cells were incubated at 37 °C in a humidified 5% CO_2 atmosphere. Cells were split by using trypsin/EDTA solution when almost confluent.

2.3 Synthesis of *N*,*N*′-bis(acryloyl) cystamine (BAC)

The *N*,*N*′-bis(acryloyl) cystamine (BAC) was synthesized according to the previous literature.[26] Briefly, cystamine dihydrochloride (10 mmol) was dissolved in a mixture of 15 mL of 3.5 M NaOH and 10 mL chloroform. This solution was heated to 50 °C, and 5 mL of chloroform containing 20 mmol of acryloyl chloride was added dropwise under constant stirring over 15 min while the reaction temperature was maintained at *ca.* 50 °C. After separating the phases while still warm, the aqueous phase was discarded. The remaining organic phase was cooled down to room temperature, and the product precipitated directly from the solution. The white crystal product was recovered by filtration and recrystallized from chloroform to give a yield of 50%.

2.4 Synthesis of disulfide-linked poly(amido amine) (SS–PAA)

As shown in Fig. 1, the disulfide-linked poly(amido amine) (SS–PAA) was synthesized by the Michael addition polymerization between propargyl amine and BAC.[27] Firstly, BAC (2.60 g, 10 mmol) and propargyl amine (550.8 mg, 10 mmol) were added into a flask and then dissolved in 20 mL MeOH. The solution was mechanically stirring at room temperature in the dark under a nitrogen atmosphere for 7 days. Then, excess propargyl amine (10 mol%) was added into the reaction solution to consume any unreacted acrylamide groups, and the reaction was performed at room temperature for at least an additional one week. Finally, the reaction solution was evaporated, and then the residue was dried in vacuum at 40 °C to give the SS–PAA containing alkyne focal groups.

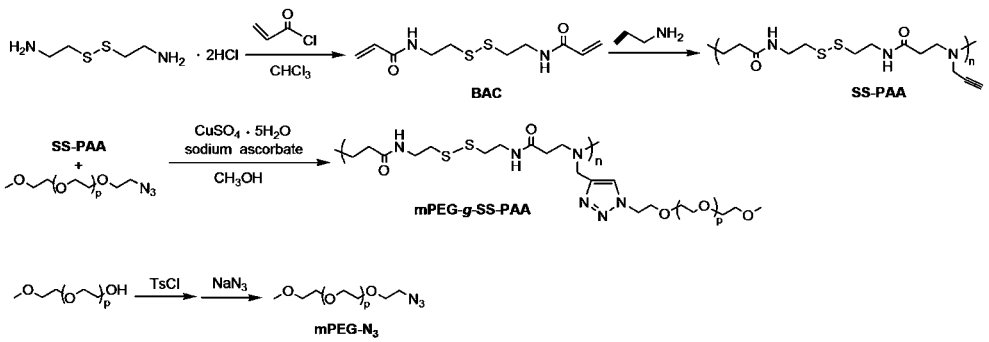

Fig. 1 Synthesis scheme of poly(ethylene glycol) monomethyl ether]-*graft*-[disulfide-linked poly(amido amine)] (mPEG-*g*-SS–PAA).

2.5 Synthesis of mPEG-*g*-SS–PAA copolymer

The mPEG-*g*-SS–PAA copolymer was synthesized by a click reaction between alkyne focal groups in SS–PAA and azide-terminated mPEG (mPEG–N_3).[28] Herein, the mPEG–N_3 was prepared from poly(ethylene glycol) methyl ether according to the previous literatures.[29] A representative procedure for the click conjugation is as follows: SS–PAA (315.46 mg, 1 mmol acetylene) and mPEG–N_3 (2.33 g, 1.2 mmol) were firstly dissolved in MeOH; subsequently, sodium ascorbate (95.10 mg, 0.48 mmol) and copper (II) sulfate pentahydrate (120.0 mg, 0.48 mmol) were added into the reaction vessel, and then was mechanically stirred at room temperature for 48 h; the crude reaction mixture was dialyzed against distilled water for 7 days using a dialysis membrane (MWCO: 3500 Da) to remove excess mPEG–N_3 and other by-products followed by lyophilizing. To adjust the polydispersity index (PDI) of the graft copolymer, the lyophilized graft copolymer was further purified by reprecipitation 5 times. Methyl alcohol and ethyl ether were used as solvent and precipitant, respectively. The resultant graft copolymer was dried in vacuum to yield 2.08 g of mPEG-*g*-SS–PAA (yield: 92%).

2.6 Characterizations of polymers

^{1}H nuclear magnetic resonance (^{1}H NMR) spectra were recorded on a Bruker Avarice ™ 500 NMR spectrometer, and the sample concentration was 35 mg mL^{-1} in DMSO-d_6 or $CDCl_3$. Fourier transform infrared (FT-IR) spectra were recorded on a Nicolet Nexus 670 spectrometer in the range of 4000–400 cm^{-1} with use of a KBr pellet.

The molecular weight and its distribution of polymers were measured with Agilent 1200 gel permeation chromatography (GPC) (Agilent Technologies Inc. Shanghai Branch). Agilent 1200 refractive index detector and aqueous SEC start-up kit were used. Chromatography columns (PL aquagel-OH MIXED columns, Polymer Laboratories Ltd. Amherst, MA, USA) were calibrated with poly(ethylene glycol) kit and polystyrene kit for different mobile phase, respectively. The column temperature was maintained at 25 °C. Mobile phases were phosphate buffer (PBS) for mPEG-*g*-SS–PAA and tetrahydrofuran (THF) for SS–PAA, respectively, and the flow rate was 1.0 mL min^{-1}.

2.7 Reduction-degradation of mPEG-*g*-SS–PAA

The degradation behavior of mPEG-*g*-SS–PAA was investigated in the presence of water-soluble reducing agent, such as dithiothreitol (DTT).[30] The concentrations of DTT in initial polymer solutions were given as 40, 20 and 10 mM, respectively. Firstly, the mPEG-*g*-SS–PAA was treated with DTT in PBS buffer under a nitrogen atmosphere at 37 °C. Aliquots were periodically withdrawn, and analyzed by GPC to determine the molecular weight and its distribution of degraded fragments after dilution with PBS buffer. Before measurement, the solution after reduction degradation was dialyzed against distilled water for 7 days using a dialysis membrane (MWCO: 1000 Da) to remove the excess DTT. At the same time, the structure of degraded fragment was determined by ^{1}H NMR while the transition from the mPEG-*g*-SS–PAA copolymer to small molecules, named as the degradation rate in this work, was obtained from the decreasing percentage of the peak area assigned to the original copolymers.

2.8 Preparation of supramolecular hydrogels

Supramolecular hydrogels based on mPEG-*g*-SS–PAA and α-CD were prepared according to formulations listed in Table 1, where some systems contained various loading-levels of DTT as reduction reagent. Generally, 200 mg α-CD was firstly dissolved into 1 mL of deionized water, and then mixed with 1 mL aqueous solution containing mPEG-*g*-SS–PAA (40 mg, equal to 0.018 mmol disulfide bonds). The ultimate concentrations of α-CD and mPEG-*g*-SS–PAA in the mixture were fixed to be of 100 mg mL^{-1} and 20 mg mL^{-1}, respectively. The resulting mixture was vigorously stirred for a while followed by sonication for 10 min, and finally conditioned at room temperature. The gelation time was settled at the time point when the mixing solution became an immobile gel in the inverted cuvettes.

Considering that such supramolecular hydrogels can be used to regulate the drug release behavior under the condition of low GSH concentration, such as extracellular milieus in the normal tissue of the human body, the DTT, as a reducing agent model and a substitute of GSH, was designatedly introduced into this kind of reduction-sensitive supramolecular hydrogels at the stage of mixing α-CD with mPEG-*g*-SS–PAA. The addition amount of DTT was given to produce the molar ratio of DTT *vs.* disulfide

Table 1 Compositions and gelation time of the mixing aqueous solution containing mPEG-*g*-SS–PAA, α-CD and DTT

	Compositions			
Sample code	α-CD (mg mL^{-1})	mPEG-*g*-SS–PAA (mg mL^{-1})	DTT/disulfide bond molar ratio	Gelation time (min)[a]
Gel/DTT-0	100	20	No DTT	10
Gel/DTT-1	100	20	1 : 1	15
Gel/DTT-5	100	20	5 : 1	25
Gel/DTT-10	100	20	10 : 1	40
Sol/DTT-25	100	20	25 : 1	No gelation
Sol/DTT-50	100	20	50 : 1	No gelation
Sol/DTT-100	100	20	100 : 1	No gelation

[a] The gelation time was settled at the time point when the mixture solution became an immobile gel in the inverted cuvettes.

bond as100 : 1, 50 : 1, 25 : 1, 10 : 1, 5 : 1 and 1 : 1, respectively. Fortunately, when the molar ratio of DTT *vs.* disulfide bond was lower than 10 : 1, the mixture composed of α-CD, mPEG-*g*-SS–PAA and DTT could result in gelation in spite of inevitable cleavage of part of the disulfide linkage. Meanwhile, a higher molar ratio of DTT *vs.* disulfide bond prolonged the gelation time.

2.9 Characterizations of supramolecular hydrogels

X-ray diffraction (XRD) measurement of the freeze-dried hydrogel powder was performed on a D/max-250 X-ray diffractometer (Rigaku Denki, Japan) equipped with a Cu Kα radiation source ($\lambda = 0.154$ nm). The diffraction data were collected in a range of $2\theta = 5$–$60°$ using a fixed time mode with a step interval of 0.02°. At the same time, the systems where the molar ratio of DTT *vs.* disulfide bond was higher than 10 : 1, were also freeze-dried as powders, and then analysed by XRD measurements.

The rheological behaviors of supramolecular hydrogels were measured on an AR 2000ex rheometer (TA Instruments, USA) using parallel plate geometry with a diameter of 60 mm at 25 °C. The gap distance between two plates was fixed at 1 mm. A frequency sweep test was conducted on each sample to determine values of storage modulus (G') and loss modulus (G'') over a frequency (ω) range of 0.1–200 rad s^{-1}. The steady flow behaviors were performed over a shearing rate range of 0.01–50 s^{-1}. Temperature control was established by a Julabo FS 18 cooling/heating bath, and kept within ±0.5 °C over an extended time.

2.10 Drug release profiles from supramolecular hydrogels

Bovine serum albumin (BSA), as a model protein drug, was used to investigate the effect of DTT on the release profiles of supramolecular hydrogels. In the process of preparing supramolecular hydrogels with and without DTT, 6.0 mg of BSA was dissolved in 0.60 mL of phosphate-buffered saline (PBS) solution (pH 7.4) containing 90 mg of α-CD, and then mixed with 0.3 mL of PBS containing 18 mg of mPEG-*g*-SS–PAA or mPEG-*g*-SS–PAA/DTT mixture. The resulting mixture was placed into a 1 mL cuvette, and incubated in a 37 °C water bath for 1 h to form a BSA-loaded hydrogel.

For *in vitro* release studies, the cuvette containing drug-loaded hydrogel was placed in a test tube with 10 mL of PBS buffer, and then conditioned in a shaking table at 37 °C. After a given interval, 0.3 mL of buffer medium was removed to determine the absorbance at 595 nm on a UV-1900PC spectroscope (Shanghai, China), and hence calculated the concentration of released BSA. At the same time, the same volume of fresh PBS solution was added to keep the total solution volume constant.

The release profile of BSA from the supramolecular hydrogel without DTT was investigated against the PBS buffer containing 0, 10, 20 and 40 mM DTT, respectively. Moreover, the release profile of BSA from supramolecular hydrogels with molar ratios of DTT *vs.* disulfide bond as 10 : 1, 5 : 1 and 1 : 1 were also investigated against the PBS buffer without DTT.

2.11 Cell viability assays of supramolecular hydrogels

A total of 600 mg of each freeze-dried powder sample of hydrogel, 100 mg of mPEG-*g*-SS–PAA and 500 mg of α-CD were put into 5 mL of RPMI1640 cell culture medium in a 50 mL centrifuge tube, respectively, and then placed in a shaker incubator (37 °C, 60 rpm) for 2 days. After that, the media were filtered with 0.22 μm sterile filter into a sterile container and stored in a refrigerator at 4 °C before use.

L929 cells were seeded into 96-well plate at an initial density of 6×10^3 cells per well in 100 μL growth medium and incubated for 24 h to reach 80% confluency at the time of treatment. Cell culture medium was replaced by 100 μL of the extracted leached medium from the corresponding hydrogel sample, mPEG-*g*-SS–PAA and α-CD. After 48 h of incubation, the well was washed twice with PBS solution, and then, a total of 10 μL of MTT solution (0.5 mg mL^{-1} in PBS) was added into each well. After further incubation for 4 h in a CO_2 cell incubator, MTT solution was removed while 100 μL of dimethyl sulfoxide (DMSO) was added into each well. Finally, the plate was incubated for 10 min in the incubator, and then for 15 min at room temperature. The optical density was measured at 570 nm using an automatic BIO-TEK microplate reader (Powerwave XS, USA) to evaluate the metabolic activity of the cells, and the cell viability was calculated from the following equation:

$$\text{Cell viability (\%)} = \frac{\text{OD}_{\text{sample}}}{\text{OD}_{\text{control}}} \times 100\% \quad (2)$$

where OD_{sample} represents the OD value from a well treated with sample and $OD_{control}$ from a well treated with PBS buffer only. Each experiment was carried out in triplicate. Results were shown as means and corresponding standard deviations (mean ± SD).

3 Results and discussion

3.1 Structure of mPEG-*g*-SS–PAA copolymer

As shown in Fig. 1, the reduction-degradable mPEG-*g*-SS–PAA was synthesized *via* a click cycloaddition reaction between azido-terminated mPEG (PEG–N_3) and the alkyne-functionalized disulfide-linked poly(amido amine) (SS–PAA). As the precursor of synthesizing alkyne-functionalized SS–PAA, the BAC monomer was synthesized according to a classic reaction pathway with acryloyl chloride under conventional Schotten–Baumann conditions. ^{1}H NMR verified the structure of as-prepared BAC, and their detail chemical shifts were shown in Fig. 2a. The FT-IR of BAC showed the characteristic adsorption bands at 1560 cm^{-1} (N–H bending, amide II), 1650 cm^{-1} (C=O, amide I) and 3250 cm^{-1} (N–H stretching) (Fig. 3a).[31] Subsequently, the alkyne-functionalized SS–PAA was synthesized conveniently by Michael addition of molar equivalents of propargyl amine *vs.* BAC. The reaction was carried out under mechanical stirring for 7–10 days until the solution became viscous. After that, in order to consume any unreacted acrylamide groups, 10% mol excess of propargyl amine was added followed by reaction for another 7 days to terminate the polymerization with amino end-groups. The final structure of alkyne-functionalized SS–PAA was confirmed by ^{1}H NMR spectrum in Fig. 2b. The signal located at 2.23 ppm suggested the presence of

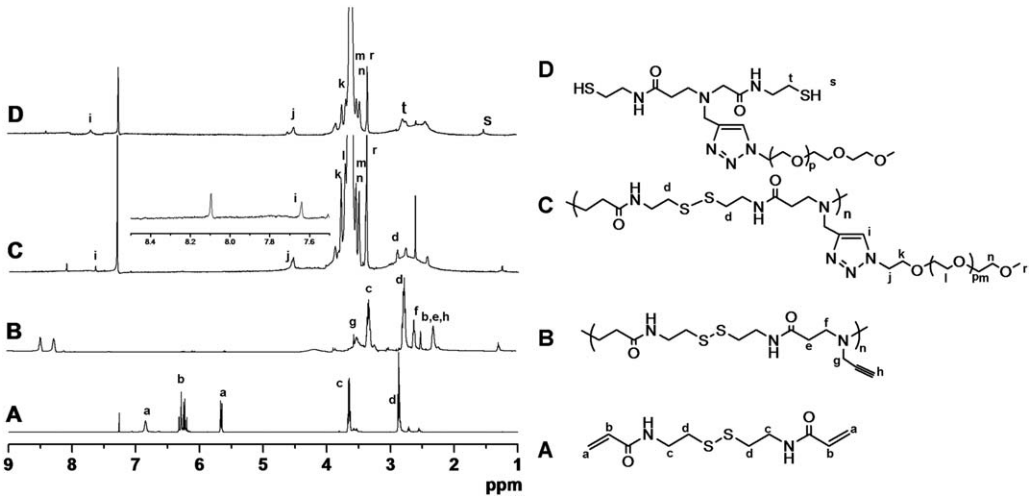

Fig. 2 ^{1}H NMR spectra of BAC in $CDCl_3$ (a), SS–PAA in DMSO-d_6 (b), mPEG-*g*-SS–PAA in $CDCl_3$ (c), and the degraded mPEG-*g*-PAA–SH in $CDCl_3$(d).

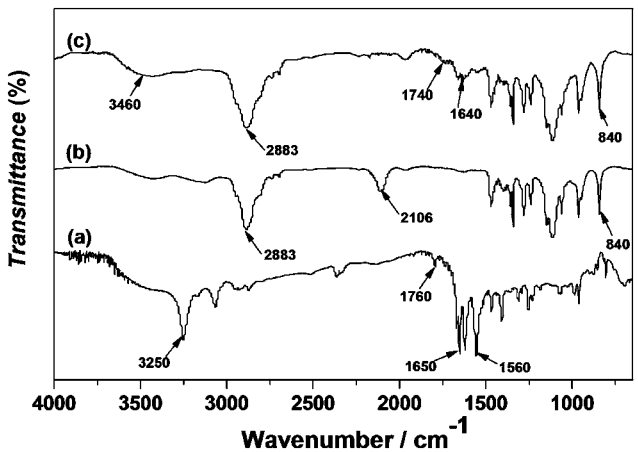

Fig. 3 FT-IR spectra of the BAC (a), mPEG–N_3 (b), and mPEG-*g*-SS–PAA (c).

alkyne focal group (–C≡CH). The weight-average (M_w) and number-average (M_n) molecular weights of alkyne-functionalized SS–PAA measured by GPC were 9.8×10^4 and 2.1×10^4, respectively. The inherent nature of the Michael addition resulted in a relatively high polydispersity index (PDI) of 4.67.

The "click" conjugation between mPEG–N_3 and alkyne-functionalized SS–PAA was carried out using $CuSO_4 \cdot 5H_2O$/sodium ascorbate as catalyst in aqueous media at room temperature. The M_w, M_n and PDI of the as-prepared mPEG-*g*-SS–PAA measured by GPC were 1.14×10^5, 5.81×10^4 and 1.98, respectively. Moreover, ^{1}H NMR confirmed the mPEG-*g*-SS–PAA structure, and the detailed signals of chemical shifts were shown in Fig. 2c. The occurrence of the "click" reaction was confirmed from the appearance of a new proton signal located at 7.64 ppm (i, singlet) and the methylene proton signal adjacent to triazole ring located at 4.53 ppm of (j, singlet) (Fig. 2c). According to the integral ratios of proton signal "i" or "j" *vs.* "c", the click conjugation between mPEG–N_3 and SS–PAA is quantitative within the error of ^{1}H NMR measurement. In addition, the FI-IR spectrum of mPEG-*g*-SS–PAA (Fig. 3c) shows a complete disappearance of the azide vibrational peak located at 2106 cm^{-1} as shown in Fig. 3b of mPEG–N_3, and a new absorption in the range of about 1600–1640 cm^{-1} for the typical character of triazole ring appeared. At the same time, the intense stretching bands at 2883 cm^{-1} and 840 cm^{-1} in Fig. 3c were assigned to grafted mPEG segments, while a broad band located in the range of 3200–3600 cm^{-1} were assigned to the –NH groups in the SS–PAA main chain.

3.2 Reduction degradation of mPEG-*g*-SS–PAA

The degradation behavior of mPEG-*g*-SS–PAA was investigated by the incubation of copolymers with DTT under physiological conditions. As previously reported,[32,33] the disulfide bonds in the SS–PAA main chain was cleaved by DTT due to the formation of more stable six-membered cyclic disulfide after the oxidation of such DTT dithiol. ^{1}H NMR and GPC measurements confirmed the cleavage of disulfide bonds to yield mPEG-*g*-PAA–SH. The new proton signal located at *ca.* 1.5 ppm (s, –SH) in Fig. 2d of mPEG-*g*-PAA–SH indicated the presence of the thiol end-group. At the same time, the ethylene protons next to the thiol end-group (–CH_2–SH) were shown as new peaks located at *ca.* 2.75 ppm while the signal intensity of methylene protons neighboring the disulfide bond (–CH_2–SS–CH_2–) located at *ca.* 2.92 ppm weakened in Fig. 2d in contrast with those in Fig. 2a, 2b and 2c. In addition, the changes of the GPC curves shown in Fig. 4a also verified the degradation process of mPEG-*g*-SS–PAA under a DTT concentration of 40 mM. As the incubation time prolonged, the peak intensity of small molecules, corresponding to *ca.* 9 min of elution time, gradually increased together with the decrease of peak proportion assigned to polymer or high molecular weight fraction. It proved that the mPEG-*g*-SS–PAA could be cleaved as a short segment, oligomer or small molecule under high reductant concentration. At the incubation time of 6 days, the GPC result showed that the high molecular-weight fraction after degradation had a M_w of 3.0×10^3, M_n of 2.88×10^3 and a PDI of 1.03. With a decrease of the DTT concentration in the incubation media, the degradation rate of mPEG-*g*-SS–PAA decreased as shown in Fig. 4b. The faster transition from

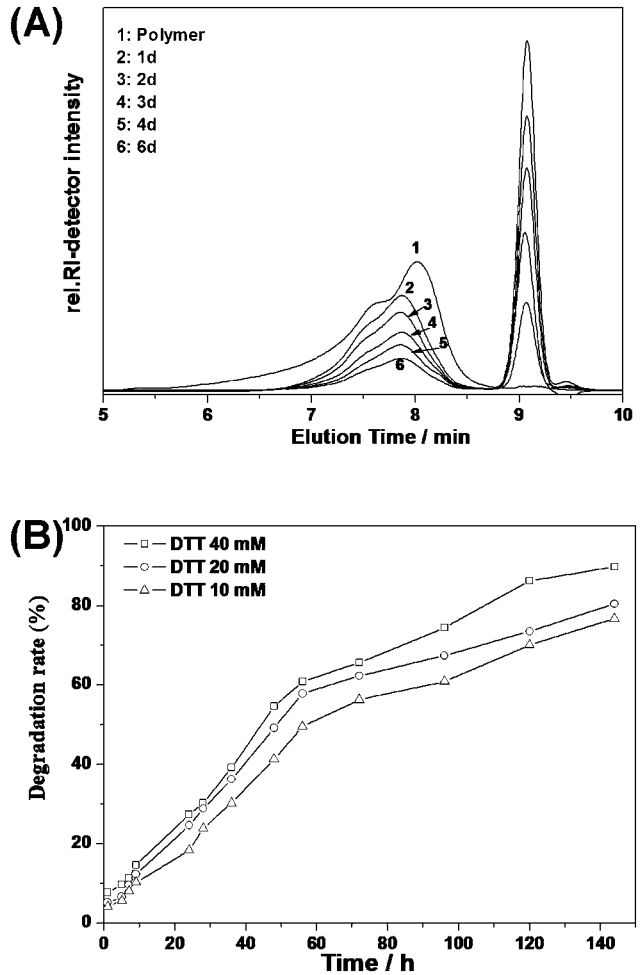

Fig. 4 GPC curves at the given time (A) of mPEG-*g*-SS–PAA incubated in PBS buffer (pH = 7.4) containing 40 mM DTT at 37 °C, and the degradation rate (B) of mPEG-*g*-SS–PAA incubated in PBS buffer (pH = 7.4) containing various DTT concentrations at 37 °C.

polymer to small molecules, named as the biodegradation of polymer in this work, was ascribed to that more amount of DTT might provide more chance to cleave the disulfide bonds of the main chain in the mPEG-*g*-SS–PAA copolymer. The highest DTT concentration of 40 mM could give the degradation of over *ca.* 90% mPEG-*g*-SS–PAA in 6 days. Although the degradation rate of mPEG-*g*-SS–PAA was obviously slower than those of other reports,[25] such reduction sensitivity still showed a potential to regulating the hydrogel structure and drug release profile. In this case, a slower degradation rate might be ascribed to the steric hindrance of grafted mPEG segments which inhibited the thiol–disulfide exchange reaction between DTT and disulfide bonds in the SS–PAA main chain.

3.3 Fabrication of supramolecular hydrogels

Based on the inclusion between α-CD and grafted mPEG segment, the mixture of mPEG-*g*-SS–PAA and α-CD in aqueous solution could form the hydrogel in tens of minutes depending upon the molar ratios of incorporated DTT *vs.* disulfide bond in mPEG-*g*-SS–PAA. The gelation time of supramolecular hydrogels with various molar ratios of DTT *vs.* disulfide bond was listed in Table 1. Obviously, the incorporation of DTT resulted in the prolongation of gelation time. With an increase in the molar ratios of DTT *vs.* disulfide bond from 1 : 1 to 10 : 1, the gelation time increased due to partial cleavage of disulfide bond in the main chain of mPEG-*g*-SS–PAA. When the molar ratio of DTT *vs.* disulfide bond was higher than 25 : 1, the severe breakage of the main chain in mPEG-*g*-SS–PAA inhibited the formation of hydrogels. Only a turbid or transparent solution was observed.

As well-known, the aggregation of (pseudo)polyrotaxanes that formed by the threading of cyclodextrin onto polymer chains, plays a key role as physical crosslinking to construct the hydrogel network. Furthermore, for those PEG segments with low molecular weight that cannot become a gelation solely, the branched structure, such as grafted comb-type[20–23] and high-densely double-grafted brush,[19] provide a possibility to gelation *via* cyclodextrin inclusion. As a result, in the system of mPEG-*g*-SS–PAA and α-CD, the aggregation of the inclusion complex between α-CD and grafted PEG segment was a driving force to induce gelation; it was proved by the XRD patterns in Fig. 5. Different from two diffraction peaks of PEG crystalline located at 18.9° and 23.5° of 2θ for mPEG-*g*-SS–PAA and the diffraction pattern of pristine α-CD, all the freeze-dried powders, including the mPEG-*g*-SS–PAA/α-CD hydrogels with or without DTT and the mPEG-*g*-SS–PAA/α-CD mixture containing a high molar

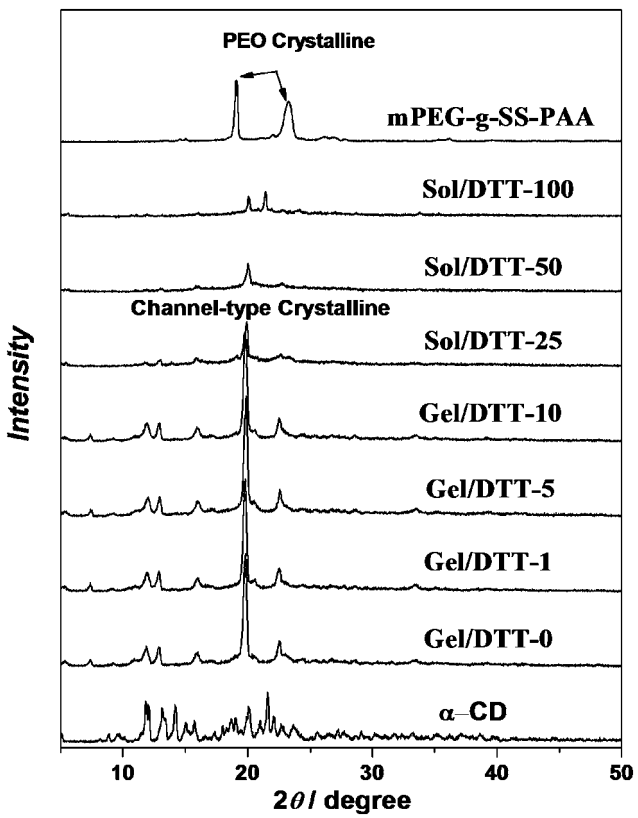

Fig. 5 XRD patterns of the powders freeze-dried from the α-CD/mPEG-*g*-SS–PAA hydrogels with and without DTT and the mixing solution containing high DTT loading-level, and the powders of α-CD and mPEG-*g*-SS–PAA as a comparison.

ratio of DTT *vs.* disulfide bond (higher than 25 : 1), showed a typical diffraction peak located at 19.7° of 2θ assigned to the "channel"-type crystalline of the PEG/α-CD pseudopolyrotaxanes.[19,20,22,23] However, when the molar ratio of DTT *vs.* disulfide bond was higher than 25 : 1, the diffraction intensities of the peak located at 19.7° of 2θ obviously weakened, suggesting that the cleavage of the SS–PAA main chain inhibited the positive effect of origin comb-like structure on improving the aggregation of pseudopolyrotaxanes and subsequently driving gelation. It is well consistent with the observation of no gelation for the mPEG-*g*-SS–PAA/α-CD system containing more DTT (the molar ratio of DTT *vs.* disulfide bond higher than 25 : 1). Fortunately, the systems with the relatively low molar ratio of DTT *vs.* disulfide bond (*i.e.* lower than 10 : 1) still became gelation, and might facilitate to extending the applications of this kind of reduction-sensitive supramolecular hydrogel as a drug carrier with a function of regulating release behavior in the condition of lower GSH concentration.

3.4 Rheological studies of supramolecular hydrogels

Rheology measurements can evaluate two fundamental properties for this category of injectable hydrogel, *i.e.* mechanical strength and shear-thinning behavior. Fig. 6a depicts the dynamic rheological behaviors of supramolecular hydrogels with and without DTT. The storage modulus (G') of all the hydrogels exhibited a substantial elastic response, and was greater than the loss modulus (G'') over the entire range of testing frequencies. It suggested that these supramolecular hydrogels possessed a permanent network, in spite that the network framework was supported by the physical interactions, and hence displayed strength and rigidity. At the same time, with an increase in the molar ratio of DTT *vs.* disulfide bond, both the G' and G'' plateaus slightly shifted downward. It is ascribed to the degradation of the SS–PAA main chain after introducing DTT. At this time, the chemical joints along the main chain in the hydrogel network were cleaved, and hence decreased the mechanical strength to some extent.

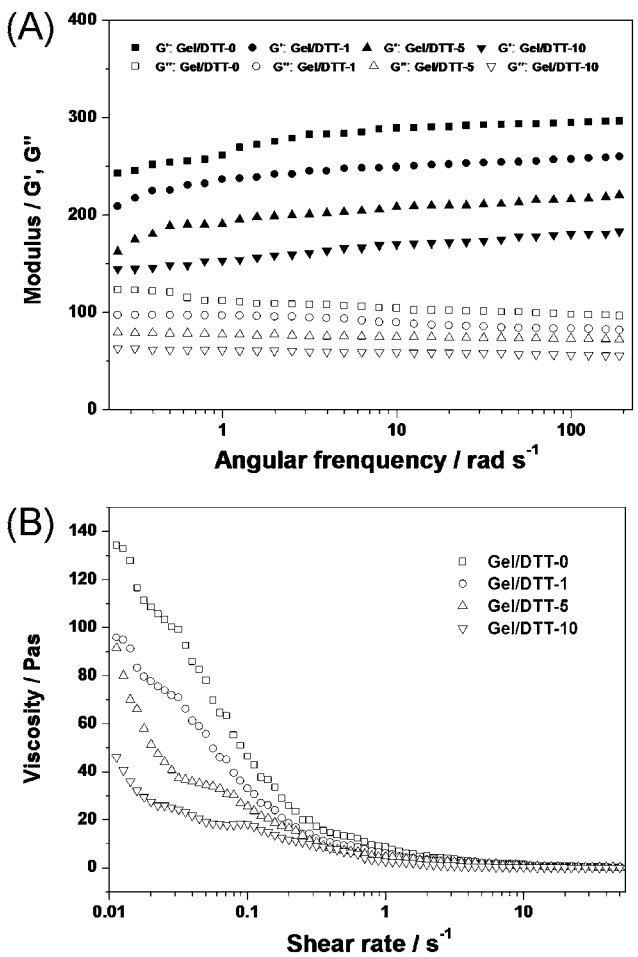

Fig. 6 Dynamic (A) and steady (B) rheological behaviors of the α-CD/mPEG-*g*-SS–PAA hydrogels with various molar ratios of DTT *vs.* disulfide bonds.

Fig. 6b depicts the steady rheological behaviors of supramolecular hydrogels with and without DTT. With an increase in shearing rate, the viscosity of all the hydrogel diminished greatly until the viscosity was almost absence at a shearing rate of 1 s^{-1}, suggesting that these supramolecular hydrogels were thixotropic. When the shearing force was removed, the flowable sols could recover the same as the hydrogel did. Such reversible gel–sol transition induced by shearing, similar to previous reports,[5–13,15–18] was a key for the application as an injectable biomaterial. In addition, the loading-level of DTT still showed the significant effect on the viscosity values of these supramolecular hydrogels. Furthermore, the dependence of the initial viscosity upon the loading-level of DTT was similar to that of the G' value, namely the initial viscosity decrease with an increase in the molar ratio of DTT *vs.* disulfide bond.

3.5 Drug release profiles of supramolecular hydrogels

Bovine serum albumin (BSA) as a model protein drug was encapsulated into the hydrogels to investigate *in vitro* release kinetics. Fig. 7a shows the effects of the DTT concentrations in testing reduction media (PBS buffer with pH 7.4) on the BSA release from the selected mPEG-*g*-SS–PAA/α-CD hydrogels without DTT. In the PBS buffer with pH 7.4, the release profile of BSA-loaded supramolecular hydrogel without DTT showed a prominent sustained release characteristic, and the accumulative release ratio was only *ca.* 70% until 30 days. With an increase of DTT concentrations in testing reduction media, the release rate of drug obviously increased. Even when the DTT concentrations were 20 and 40 mM, the test was carried out only in 22 and 18 days because the severe degradation of mPEG-*g*-SS–PAA while the accumulative release ratio was close to 100%.

As mentioned in the introduction, the disulfide bonds show enough stability in the body circulation and in the extracellular milieus due to the low concentration of reducing agent, *i.e.* glutathione tripepetide (GSH). As a result, the DTT, a reducing agent model and a substitute of GSH, was designatedly incorporated into the supramolecular hydrogel to regulate the drug release behavior. The release profiles of BSA from the supramolecular hydrogels with various molar ratios of DTT *vs.* disulfide bonds were investigated against the PBS buffer with pH 7.4. Fig. 7b depicted the effects of the molar ratios of DTT *vs.* disulfide bonds on the release process of BSA from supramolecular hydrogel containing DTT. Remarkably, a higher molar

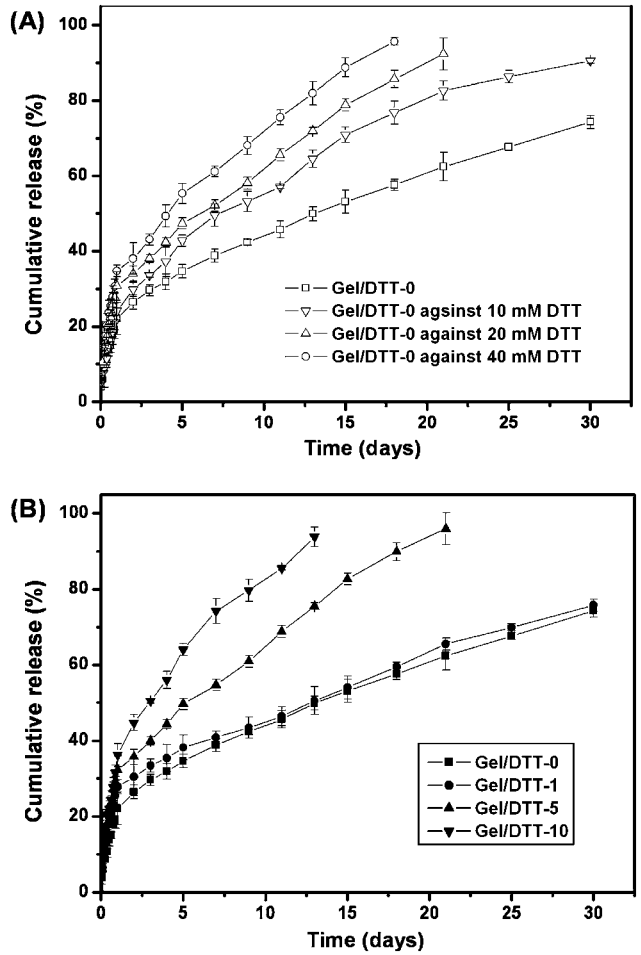

Fig. 7 *In vitro* release profiles of BSA from the α-CD/mPEG-*g*-SS–PAA hydrogels against PBS buffer of pH = 7.4 containing various DTT concentrations (A) and from the α-CD/mPEG-*g*-SS–PAA hydrogels with various the molar ratio of DTT *vs.* disulfide bond against PBS buffer of pH = 7.4 (B).

ratio of DTT *vs.* disulfide bond, corresponding to more DTT in the supramolecular hydrogel, resulted in a higher release rate of BSA. When the molar ratio of DTT *vs.* disulfide bond was 10 : 1, over 90% BSA was released only in 15 days. It was ascribed to the rapid erosion of the supramolecular hydrogel due to the severe cleavage of mPEG-*g*-SS–PAA under high reductant concentration. Since the incorporation of proper DTT loading-level could still produce supramolecular hydrogel and show the ability to regulating the drug release as expected, this strategy might extend the application of such reduction-sensitive supramolecular hydrogels.

3.6 Cytotoxicity of supramolecular hydrogels

Combined with injection potential and good sustained release profile, this kind of reduction-sensitive supramolecular hydrogel may be considered as an injectable smart biomaterial. As a result, to know their cytotoxicity as the elementary evaluation of biocompatibility, the *in vitro* cell viability of the extracted leached media from supramolecular hydrogel as well as mPEG-*g*-SS–PAA and α-CD was evaluated by the MTT assay using L-929 cell line. Fig. 8 depicts the dependence of cell viability upon the testing concentrations for mPEG-*g*-SS–PAA, α-CD and the freeze powder of supramolecular hydrogel without DTT, and it was shown as representative concentration–growth inhibition curves. When the testing concentration of the freeze-dried powder of supramolecular hydrogel was lower than 60 mg mL^{-1},

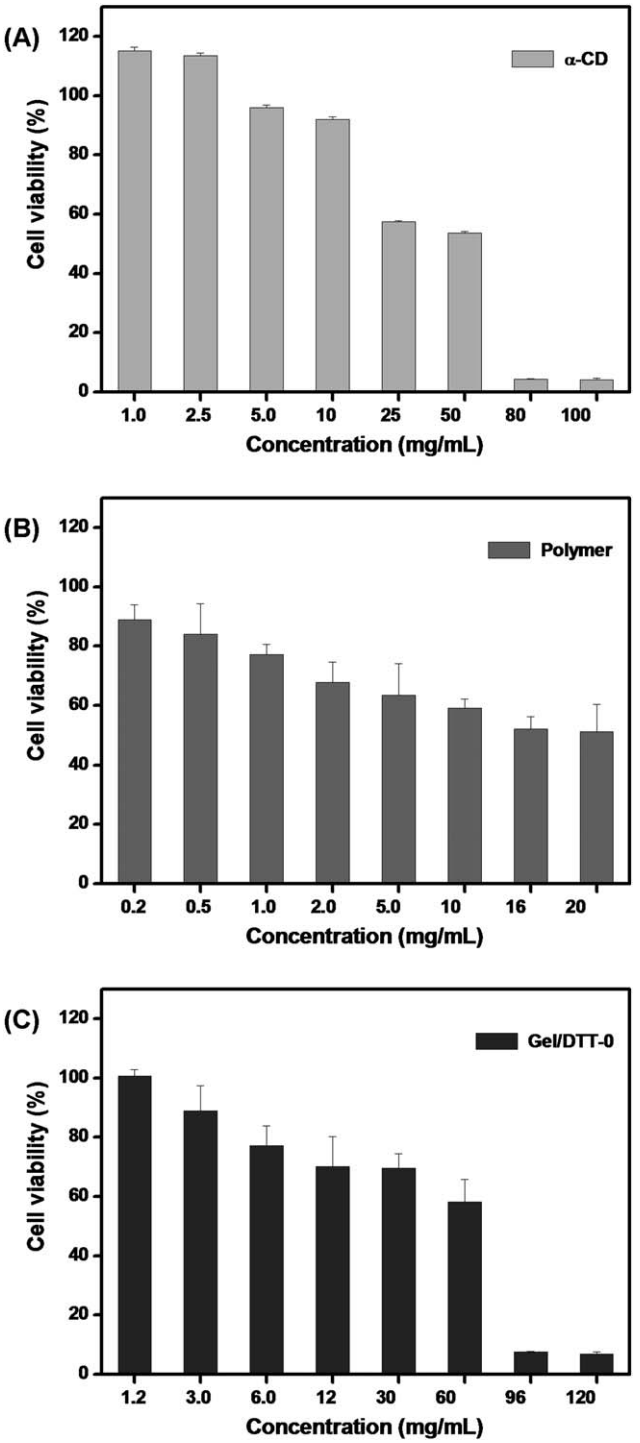

Fig. 8 Cell viability of the freeze-dried powder of α-CD/mPEG-*g*-SS–PAA hydrogel (C) at various concentrations as well as α-CD (A) and mPEG-*g*-SS–PAA (B) at equivalent concentrations against L929 cell line for 48 h.

the freeze-dried powder of supramolecular hydrogel without DTT as well as the mPEG-*g*-SS–PAA and α-CD with the equivalent concentrations inhibited cell growth in a dose-dependent manner, and showed equivalent cell viability at the same equivalent concentrations. In particular, the cell viability for the freeze-dried powder of supramolecular hydrogel without DTT was close to 100% for low concentrations of 1.2 and 3.0 mg mL^{-1}. However, when the testing concentration for the freeze-dried powder of supramolecular hydrogel without DTT was higher than 90 mg mL^{-1}, the supramolecular hydrogel without DTT showed the cell viability of less than 10% due to the severe cytotoxicity of high α-CD concentration.[34] The severe cytotoxicity of high equivalent concentration of α-CD was also depicted by the results in Fig. 8a. In virtue of infinite diluted condition in body circulation, such reduction-sensitive supramolecular hydrogel might meet the requirement of low cytotoxicity as an injectable biomaterial.

4 Conclusions

Based on the design of molecular structure, the reduction-sensitive disulfide bond and the included poly(ethylene glycol) (PEG) segments were combined together to synthesize [PEG monomethyl ether]-*graft*-[disulfide-linked poly(amido amine)] (mPEG-*g*-SS–PAA). Moreover, the inclusion of α-cyclodextrin (α-CD) to PEG segments induced the formation of supramolecular hydrogels. Such supramolecular hydrogels inherited the shear-thinning character and reduction-sensitivity, and showed an adjustable sustained drug-release characteristic depending upon the reduction condition. Fortunately, low loading-level of reducing agent cannot inhibit the formation of hydrogel, and provided a possibility of regulating drug release profile in extracellular milieus and normal tissue. This is the first report on reduction-sensitive supramolecular hydrogel based on cyclodextrin/polymer inclusion. Consideration of their acceptable cytotoxicity, such reduction-sensitive supramolecular hydrogels showed a great potential as an injectable smart biomaterial for the application of drug controlled-release.

Acknowledgements

The research work was financially supported by 973 Projects of Chinese Ministry of Science and Technology (2009CB930300); Foundation of Shanghai Municipality Commission (10410710000, 09540709000); Fundamental Research Funds for the Central Universities (Self-Determined and Innovative Research Funds of WUT 2010-II-022); and Open Project of Chinese Academy of Sciences Key Laboratory of Biological Effects of Nanomaterials and Nanosafety.

References

1 J. Li, *Adv. Polym. Sci.*, 2009, **222**, 79–113.
2 F. van de Manakker, T. Vermonden, C. F. van Nostrum and W. E. Hennink, *Biomacromolecules*, 2009, **10**, 3157–3175.
3 J. Li and X. J. Loh, *Adv. Drug Delivery Rev.*, 2008, **60**, 1000–1007.
4 I. I. Abu Hashim, T. Higashi, T. Anno, K. Motoyama, A. E. H. Abd-Elgawad, M. H. El-Shabouri, T. M. Borg and H. Arima, *Int. J. Pharm.*, 2010, **392**, 83–91.
5 Y. Chen, X. H. Pang and C. M. Dong, *Adv. Funct. Mater.*, 2010, **20**, 579–586.
6 X. L. Zhang, J. Huang, P. R. Chang, J. L. Li, Y. M. Chen, D. X. Wang, J. H. Yu and J. H. Chen, *Polymer*, 2010, **51**, 4398–4407.
7 X. P. Ni, A. Cheng and J. Li, *J. Biomed. Mater. Res., Part A*, 2009, **88A**, 1031–1036.
8 S. P. Zhao, J. Lee and W. Xu, *Carbohydr. Res.*, 2009, **344**, 2201–2208.
9 L. X. Ren, L. H. He, T. C. Sun, X. Dong, Y. M. Chen, J. Huang and C. Wang, *Macromol. Biosci.*, 2009, **9**, 902–910.
10 D. Wu, T. Wang, B. Lu, Z. D. Xu, S. X. Cheng, X. J. Jiang, X. Z. Zhang and R. X. Zhuo, *Langmuir*, 2008, **24**, 10306–10312.
11 X. Li and J. Li, *J. Biomed. Mater. Res., Part A*, 2008, **86A**, 1055–1061.
12 J. Li, X. Li, X. Ni, X. Wang, H. Li and K. W. Leong, *Biomaterials*, 2006, **27**, 4132–4140.
13 J. Li, X. Ni and K. W. Leong, *J. Biomed. Mater. Res., Part A*, 2003, **65A**, 196–202.
14 T. Wang, X. J. Jiang, Q. Z. Tang, X. Y. Li, T. Lin, D. Q. Wu, X. Z. Zhang and E. Okello, *Acta Biomater.*, 2009, **5**, 2939–2944.
15 K. L. Liu, J. L. Zhu and J. Li, *Soft Matter*, 2010, **6**, 2300–2311.
16 S. P. Zhao, L. M. Zhang and D. Ma, *J. Phys. Chem. B*, 2006, **110**, 16503–16507.
17 S. P. Zhao, L. M. Zhang and D. Ma, *J. Phys. Chem. B*, 2006, **110**, 12225–12229.
18 J. Li, X. Li, Z. Zhou, X. Ni and K. W. Leong, *Macromolecules*, 2001, **34**, 7236–7237.
19 L. H. He, J. Huang, Y. M. Chen, X. J. Xu and L. P. Liu, *Macromolecules*, 2005, **38**, 3845–3851.
20 K. M. Huh, Y. W. Cho, H. Chung, I. C. Kwon, S. Y. Jeong, T. Ooya, W. K. Lee, S. Sasaki and N. Yui, *Macromol. Biosci.*, 2004, **4**, 92–99.
21 H. S. Choi, K. Kontani, K. M. Huh, S. Sasaki, T. Ooya, W. K. Lee and N. Yui, *Macromol. Biosci.*, 2002, **2**, 298–303.
22 K. M. Huh, T. Ooya, W. K. Lee, S. Sasaki, I. C. Kwon, S. Y. Jeong and N. Yui, *Macromolecules*, 2001, **34**, 8657–8662.
23 H. S. Choi, K. Yamamoto, T. Ooya and N. Yui, *ChemPhysChem*, 2005, **6**, 1081–1086.
24 R. X. Yuan and X. T. Shuai, *J. Polym. Sci., Part B: Polym. Phys.*, 2008, **46**, 782–790.
25 F. Meng, W. E. Hennink and Z. Zhong, *Biomaterials*, 2009, **30**, 2180–2198.
26 H. Yu and D. W. Grainger, *Macromolecules*, 1994, **27**, 4554–4560.
27 C. Lin, C. J. Blaauboer, M. M. Timoneda, M. C. Lok, M. van Steenbergen, W. E. Hennink, Z. Zhong, J. Feijen and J. F. J. Engbersen, *J. Controlled Release*, 2008, **126**, 166–174.
28 B. Parrish and T. Emrick, *Bioconjugate Chem.*, 2007, **18**, 263–267.
29 C. Hua, S. M. Peng and C. M. Dong, *Macromolecules*, 2008, **41**, 6686–6695.
30 Y. Sun, X. L. Yan, T. M. Yuan, J. Liang, Y. J. Fan, Z. W. Gu and X. D. Zhang, *Biomaterials*, 2010, **31**, 7124–7131.
31 H. Yu and D. W. Grainger, *Macromolecules*, 1994, **27**, 4554–4560.
32 N. V. Tsarevsky and K. Matyjaszewski, *Macromolecules*, 2002, **35**, 9009–9014.
33 H. L. Fan, J. Huang, Y. P. Li, J. H. Yu and J. H. Chen, *Polymer*, 2010, **51**, 5107–5114.
34 J. C. Debouzy, F. Fauvelle, S. Crouzy, L. Girault, Y. Chapron, M. Göschl and A. Gadelle, *J. Pharm. Sci.*, 1998, **87**, 59–66.

